# The Extent of Previously Unknown Coral Communities in the Burnett-Mary Region (Southeast Queensland)

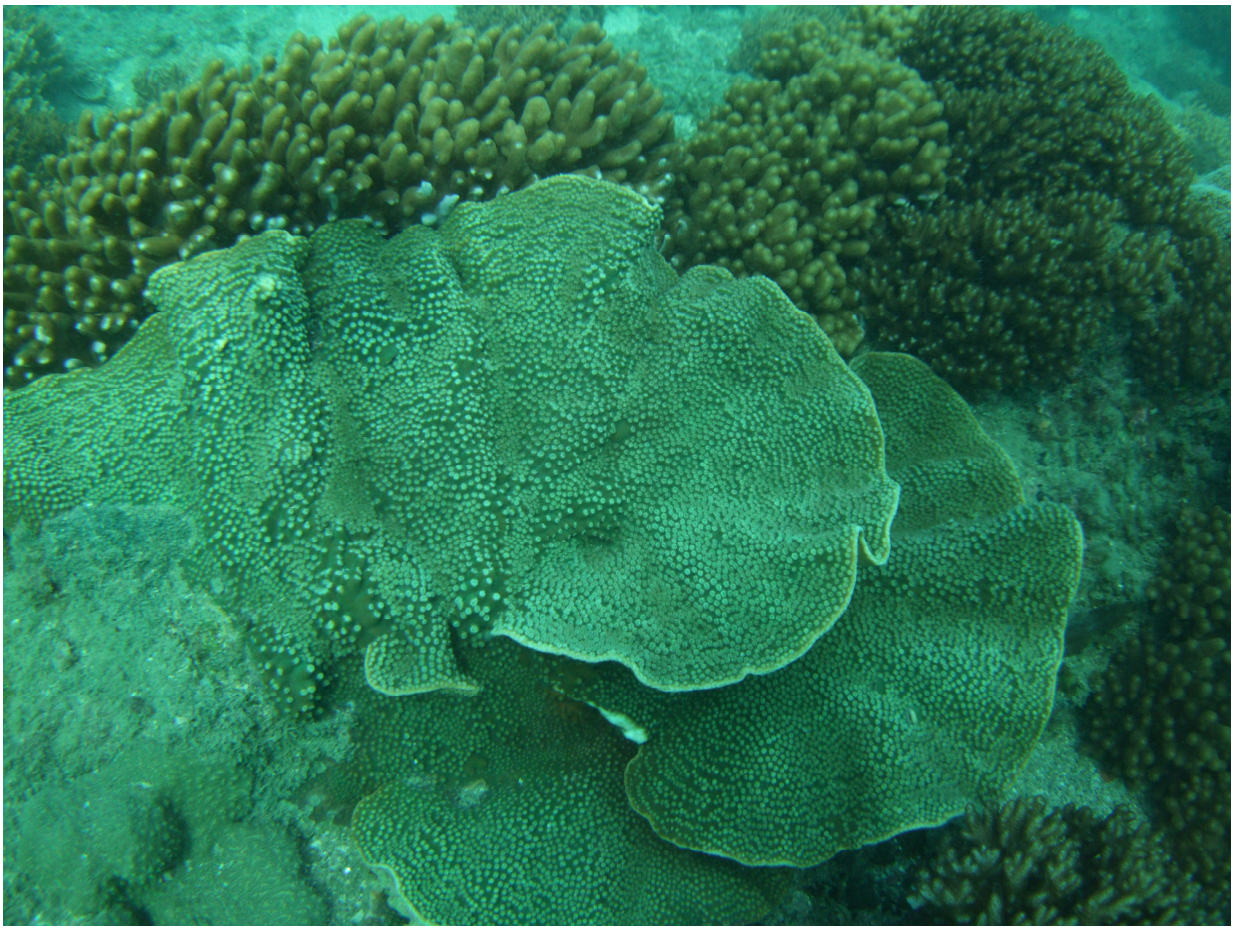

**ABSTRACT**

The Burnett Mary region is located along the southern Queensland coast and supports a broad range of benthic reef communities. This region is positioned within a biogeographical overlap zone, containing a unique assemblage of tropical, subtropical and possibly temperate species near their latitudinal limits. These marine communities are subject to a range of natural and anthropogenic disturbances occurring at a variety of temporal and spatial scales. The aim of this study is to assess the extent of benthic communities in the region as a baseline against which future changes can be monitored. The photo transect and remote sensing technique employed to survey these benthic communities occurred during 2008/2009. Soft corals were the dominant benthos with *Lobophyton spp* the most numerous. Scleractinean corals were represented by *Acropora spp.* and *Pocillopora damicornis*, a moderate to low cover of *Goniopora spp., Montipora spp.* and *Turbinaria spp*. were also recorded at most of the survey sites. The long-term monitoring of these benthic communities is essential to improve our understanding of the temporal variations occurring within this region and on broader spatial scales, as well as to assess the effects of natural and anthropogenic disturbances. This information can in turn, be used to develop more effective management strategies that will attempt to mitigate long-term damage to these benthic reef communities.

Key Words: Reef communities, corals, benthic structure, extent.

**INTRODUCTION**

Of the world's coral reef ecosystems, it has been estimated that 20% have been destroyed, 24% are degraded, while another 26% are seriously threatened (Wilkinson, 2004). Hence, there is an urgent need to protect and carefully manage coral reefs and coral-dominated communities. The long-term viability of coral reef ecosystems is largely dependent upon gaining an understanding of ecosystem functioning, spatial and temporal variability, natural and anthropogenic disturbance regimes, the critical thresholds of biota to such disturbances and the factors that influence recovery processes. Various studies have been

conducted on the coral reef communities north of the southern Great Barrier Reef (GBR) boundary and south of Moreton Bay. However, there is limited information on the coral communities between these two regions. In particular, there is no published literature on the benthic reef communities within the Burnett Mary region. Consequently, the extent of these communities is largely unknown.

This study was conducted to establish a baseline study on the benthic communities within the Burnett Mary region. This baseline dataset is required for the establishment of a long-term monitoring program, which will greatly improve our understanding of these northern subtropical reefs, which lie adjacent to rapidly expanding coastal regions (Banks and Harriott, 1995). In particular, these subtropical reefs are currently of high research interest with regards to quantifying the impacts of climate change in the future.

**METHODS**

Coral-dominated reefs, rocky and sandy shores, mangroves, and estuaries are the main habitats present within the Burnett Mary region (WMPMEP, 2003). However, there is no published literature on the communities within these habitats.

The coastal environment is a naturally highly dynamic system, with changes to the benthic habitats occuring on a relatively short timescale. For example, several areas clearly show reefs present in aerial photos (2001), however these reefs are no longer visible in Quickbird images taken from 2003-2008.

The following water column correction and sun glint removal algorithms reduce the effect of suspended sediments and surface roughness, but they do not remove the problems. So, there is still too much variation between post-processed images, meaning that classification schemes developed for one image could not be applied to other images. For this reason all images were processed seperately.

A) Geometric Correction

Quickbird satellite imagery data were initially geometrically corrected by the provider in order to reduce distortions which are mainly caused by scanning errors, the rotation and curvature of the Earth, and changes in altitude of the platform during data acquisition. The

datasets were georeferenced as well, based on satellite track parameters. However, the correction was not of high enough accuracy, and the images were provided in an arbitrary projection and could not be matched to a common projection. Thus, further geometric correction was required, and was applied using geometrical transformation (Jensen, 1996), based on global positioning system (GPS) ground control points (GCPs) where available (two images) or image to image transformation using coordinates from GoogleEarth (six images).

The images were projected into Universal Transverse Mercator (UTM), Zone 56 South. Because of the methodology employed in further processing, exact rectification was not required.

B) Pre-processing

All images were pre-processed to covert pixel digital numbers (DN) to satellite reflectance values (by Abdullah Habib). This is required for correct operation of other algorithms. This pre-processing function is called radiometric correction. Radiometric correction encompasses three consecutive steps (Mumby and Clark, 2000). The first step is DN conversion to spectral radiance value. This is followed by conversion of spectral radiance to the top of atmospheric (TOA) reflectance and the final step is atmospheric correction using dark subtract technique.

1. Conversion of DN to spectral radiance

The DN conversion to spectral radiance was based on the technical note from the Quickbird data provider, Digital Globe (Krause, 2005).

$$L\lambda_{Pixel,Band} = (K_{Band} * q_{Pixel,Band}) / \Delta\lambda_{Band}$$

where:

$L\lambda_{Pixel,Band}$ : top-of-atmosphere spectral radiance image pixels [W-m-2-sr-1-µm-1]

$K_{Band}$ : the absolute radiometric calibration factor [W-m-2-sr-1-count-1] for a given band

$q_{Pixel,Band}$ : radiometrically corrected image pixels [counts]

$\Delta\lambda_{Band}$ : the effective bandwidth [µm] for a given band

Table 1. Quickbird effective bandwith (after Krause, 2005)

Spectral Band  Effective bandwith (µm)

| Spectral Band | Effective bandwith (µm) |
|---|---|
| Pan | 0.398 |
| Blue | 0.068 |
| Green | 0.099 |
| Red | 0.071 |
| NIR | 0.114 |

2. Conversion of spectral radiance to spectral reflectance

Krause (2005) noted that the spectral radiance to spectral reflectance conversion technique for Quickbird imagery is similar to the technique as applied to data from other satellite platforms. The formula used in this step is:

$$\rho \lambda \text{ Pixel, Band} = [L\lambda \text{ Pixel, Band} * d \text{ ES } 2 * \pi] / [\text{Esun } \lambda \text{ Band} * \cos (SZ)]$$

where:

ρ λ Pixel, Band : reflectance at surface (range value of 0-1)

π : 3.141593

Lλ Pixel, Band : top-of-atmosphere spectral radiance image pixels [W-m-2-sr-1-µm-1]

d : earth-sun distance in astronomical units, calculated as:

$d = 1 - [0.01674 * \cos ((0.9856 * (JD - 4))]$

with JD: Julian Day of image acquisition

Esun λ Band : band-averaged solar spectral irradiance in W-m-2µm-1

SZ : Sun Zenith angle at the moment of image acquisition, calculated as:

$SZ = (90 - SE)$ )

with SE: sun elevation angle

(all cosine values are in degrees and need to be converted to radiance values by multiplying by (π / 180))

Table 2. Quickbird band-averaged solar spectral irradiance (after Krause, 2005)

Spectral Band Spectral irradiance (W-m-2µm-1)

| Spectral Band | Spectral irradiance ($W\text{-}m^{-2}\ \mu m^{-1}$) |
|---|---|
| Pan | 1381.79 |
| Blue | 1924.59 |
| Green | 1843.08 |
| Red | 1574.77 |
| NIR | 1113.71 |

3. Atmospheric correction using dark subtract technique

Atmospheric correction was applied using the dark pixel subtraction method (Chavez, 1988). This technique assumes that in each image, a dark object is present which totally absorbs the solar irradiance. If atmospheric and water surface conditions are assumed to be uniform throughout the scene, the mean deep-water radiance at sensor can be used to remove the atmospheric effect and the effect of sea-surface reflectance (Gordon and Morel, 1983; Mumby and Edwards, 2000b).

The Quickbird data available did not all have the deep-water region (more than 30m), hence a subtraction method using band minimum was applied. This technique searches for the minimum DN value (dark objects) of each spectral band in the image and uses it for the dark subtraction calculation.

C) Masking

Terrestrial and other non-oceanic features are masked to restrict the brightness value of aquatic features, and hence enhance feature discrimination (Jensen et al. 1991). All images were masked using unsupervised classification into “sea” and “non-sea” classes to determine the coastline. This coastline was used to mask out all non-sea areas, and to

apply a 1000 metre seaward buffer i.e. the area considered in this project is from the coastline extending out to sea by 1 kilometre.

D) Sun Glint Removal

Three of the Quickbird images required removal of surface roughness (sun glint). The images affected by surface roughness were processed with a deglint algorithm, to enhance below-surface information.

Sun glint appearance distorts the sea surface, especially within high resolution satellite images. This appears as a sparkling light on the water surface due to the sun elevation and inhibits detection of underwater objects. Sun glint on the water surface was removed using the Hedley et al. (2005) technique, based on the rationale that visible bands have a correlation to the Near Infra Red band. The formula used in deglinting process is:

$$R'i = Ri - bi\ (R\ NIR - Min\ NIR)$$

where:

R'i : deglinted band

Ri : unglinted band

bi : regression slope between NIR and visible band i

R NIR : NIR band

Min NIR : minimum value obtained from NIR band

E) Water column correction

All images were processed with a water column correction (WCC) algorithm to reduce the effects of suspended sediment. The light attenuation effect on the water bodies (a process where light penetration intensity decreases exponentially with increasing water depth) was removed using Lyzenga formula (1981). This formula is based on the concept that the bottom reflected radiance has a linear function of the bottom reflectance and an exponential function of the water depth.

In order to correct the effect of water column, Lyzenga (1981) suggested applying a depth invariant index formula. This is based on four processing steps; homogenous substrate at

various depth selection, ratio attenuation coefficient of a pair of bands calculation, depth and radiance linearisation, and generate a depth invariant index.

1. Selection of homogenous substrate at various depths

Lyzenga (1981) suggested selecting a uniform bottom substrate at various depths, which was then specified by Mumby and Edwards (2000b) as a preference for sandy bottom substrate as this is easier for interpreters to recognize. A true colour composite of RGB 321 was displayed and the values from three bands were extracted from the DN.

2. Calculation of the ratio attenuation coefficient of a pair of bands

Ratio attenuation coefficient was obtained using the following equations:

$$Ki/Kj = a + \sqrt{(a2 + 1)}$$

and:

$$a = \sigma ii - \sigma jj / 2 \sigma ij$$

where:

Ki/Kj : Depth invariant index

σ ii : variance of band i

σ jj : variance of band j

σ ij : covariance of band i and j

3. Linearise the relationship between depth and radiance

Increase of the depth results in the exponential function in water attenuation. In order to linearise the image (in radiance units), the natural logarithmic calculation was applied using following formula:

$$Xi = \ln (Li)$$

where:

Xi : normalised image in band i

Li : atmospheric corrected image of band i (radiance unit)

4. Generate a depth invariant index

The last step in the water column correction technique is depth invariant index of bottom type within a pair of bands, using:

depth invariant index ij = x i – [(ki / kj) * xj ]

F) Classification

The process of classification attempts to segment an image into a number of spectrally distinct groups. Each group has a particular set of homogeneous spectral characteristics called its spectral signature. Image pixels are discriminated and allocated to a specific group according to decision rules. The decision rules can be constructed automatically by the classification software (unsupervised classification) based on image statistics, or manually by the operator based on some supporting data such as field observations (supervised classification). In this case, all images were segmented using unsupervised classification, giving from 6 to 20 classes, which were given sea floor class values based on expert aerial photo interpretation. In one case (image showing Burnett Heads), the quickbird image quality was not sufficient to produce useable results, so the aerial photo interpretation was used directly to segment the image.

**2. GPS Photo Transect Technique & Survey Sites for groundthruthing satellite imagery**

The benthic reef communities within the Burnett Mary region from Hummock Hill Island in the north to Woodgate in the south were surveyed in 2008. 16 Representative sites were chosen to estimate benthic cover. These sites are Hummock Hill 1, 2, 3, Pan Cake Creek 1, 2, Burnett Heads 1, 2, 3, Burckitts reef 1, 2, Barolin 1, 2, Elliott Heads 1, 2, and Dr. Mays Island 1, 2.

The GPS photo transect technique employed during this study was based on Roelfsema et al. (2006). The results of numerous studies have proven this technique to be an efficient and effective means of quantifying benthic cover and assessing temporal and spatial variations in marine benthic communities. Furthermore, transects can be re-examined if

there is any uncertainty with identifications or if not all the required information is obtained during the initial analysis (Carleton and Done, 1995).

At each of the survey sites, random transects were photographed with a PVC tube filling the image as reference using SCUBA. A GPS on a float directly above and attached to the diver followed the tracks covered. Software GPS Photolink matched synchronized time and coordinate with each image. Photographs and specimen samples were taken for most species encountered.

3.3 Data Analysis

Subsequently, a list of benthic categories was developed and entered into the Coral Point Count with Excel extensions (CPCe) software program. The taxonomic resolution chosen for each species largely depended upon its distinctiveness. A random overlay of 20 points was created and the benthic category underlying each of the points was identified and entered into CPCe. The CPCe data files were then transferred into Microsoft Excel, which provided an automated output of the mean, standard deviation and standard error of the percentage cover of the benthic categories.

**RESULTS**

*1. Cover of benthic classes*

For detailed cover of the benthic classes see accompanying map, ARC GIS shape files and Table 3.

Table 3. Total cover of the benthic classes in the Burnett Mary region

| **Benthic class** | **Cover ($m^2$)** |
|---|---|
| Hard coral | 182,332 |
| Soft coral | 8,646,798 |

| | |
|---|---|
| Rock and rubble | 18,607,460 |
| Sea grass | 868,400 |
| Sand | 199,286,698 |
| **Total area** | **227,591,688** |

2. Species

A total of 80 coral species were encountered, of which 34 soft corals and 45 hard corals (see Table 4). Pan Caka Creek (jada's reef was covered for 95% with *Acropora* species.

Table 4. List of all species encountered (not all corals could be identified).

| **Soft Corals** |
|---|
| *Anthogorgia1* |
| *Anthogorgia2* |
| *Briaerium* |
| *Capnella* |
| *Cladiella* |
| *Cladiella/Klyxum* |
| *Cladiella?* |
| *Cladiella1* |
| *Dendronephthya* |
| *Dendronephthya1* |
| *Dendronephthya2* |
| *Faviidae1* |
| *Goniopora1* |
| *gorgonia* |
| *Hicksonella?* |
| *Isis* |
| *Isis1* |
| *Klyxum1* |
| *Klyxum2* |
| *Lobophyton* |
| *Lobophytum/Cladiella* |
| *Lobophytum1* |
| *Lobophytum1* |
| *Lobophytum2* |
| *Lobophytum3* |
| *Menella* |
| *Sarcophyton* |
| *Sarcophyton1* |
| *Sarcophytum1* |
| *Sarcophytum2* |

| |
|---|
| *Sarcophytum3* |
| *Sinularia_Dampia* |
| *Sinularia1* |
| *Sinularia2* |
| |
| **Hard Corals** |
| *blue bumpy* |
| *Braincoral* |
| *bumpy 3* |
| *Echinopora* |
| *encrusting* |
| *Encrusting blue* |
| *Favid* |
| *Faviidae2* |
| *Faviidae3* |
| *Goniastrea australensis* |
| *Hydnopora* |
| *Lobed coral* |
| *Massive* |
| *massive hard coral* |
| *Millepora* |
| *Montipora* |
| *Mussid* |
| *plate* |
| *Poccilopora* |
| *Pocillopora damicornis* |
| *Pocillopora1* |
| *Pocillopora2* |
| *Porites* |
| *Porites1* |
| *Porites2* |
| *Stylophora?* |
| *Tubipora* |
| *Turbinaria1* |
| *Turbinaria2* |
| *Unidentified Hard Coral* |
| *Unidentified Hard Coral1* |
| *Xenia* |
| *Acropora latistella* |
| *Acropora muricata* |
| *Acropora millepora* |
| *Acropora nasuta* |
| *Acropora intermedia* |
| *Acropora valida* |
| *Acropora tenuis* |
| *Acropora valida* |
| *Acropora yongei* |
| *Acropora cerealis* |
| *Acropora samoensis* |
| *Acropora muricata* |
| *Acropora digitifera* |

**REFERENCES**

Chavez, P.S. (1988). An improved dark-object subtraction technique for atmospheric scattering correction of multispectral data. Remote Sensing of Environment 24: 459-479.

Gordon, H.R. and Morel, A. Y. (1983). Remote assessment of ocean color for interpretation of satellite visible imagery: A review. Springer.

Hedley, J. D., Harborne, A. R. and Mumby, P. J. (2005). Technical note: Simple and robust removal of sun glint for mapping shallow-water benthos'. International Journal of Remote Sensing, 26:10, 2107 - 2112

Jensen, J. R., Narumalani, S., Weatherbee, O., and Mackey, H. E. (1991). Remote Sensing Offers an Alternative for Mapping Wetlands. Geo Information Systems 1:46-53.

Jensen, JR. (1996). Introductory digital image processing. A remote sensing perspective. Second edition. Prentice Hall series in Geographic Information Science. Upper Saddle River, New Jersey. Pp 316.

Krause, K. (2005). Radiometric use of Quickbird imagery – Technical Note. Digital Globe Inc., 18p.

Lyzenga, D.R. (1981) Remote sensing of bottom reflectance and water attenuation parameters in shallow water using aircraft and Landsat data. International Journal of Remote Sensing, 10, 53-69.

Mumby, P.J.; Clark, C.D. (2000). Radiometric correction of satellite and airborne images, in: Green, E.P.; Mumby, P.J.; Clark, C.D. 2000. Remote sensing handbook for tropical coastal management. Coastal Management Sourcebooks, 3. UNESCO Publishing: Paris, France. 316 pp.

Mumby, P.J. and Edwards, A.J. (2000). Water column correction techniques. In A.J. Edwards (Ed.), Remote sensing handbook for tropical coastal management (pp.121-128). Paris: UNESCO.

Banks, S.A. and Harriott, V.J. (1995). Coral communities of the Gneering Shoals and Mudjimba Island, South-eastern Queensland. Marine and Freshwater Research 46, 1137-1144.

Wilkinson, C.R. (2004). Status of Coral Reefs of the World: 2004. Australian Institute of Marine Science, Townsville.

WMPMEP (2003) Woongarra Marine Park – Park Overview [Online], Available: http://www.widebay.net/wmpme/overview.htm [24 April 2008].